Research Article | Vol. 8, No. 4 | 1 Apr 2017 | BIOMEDICAL OPTICS EXPRESS 2235
Biomedical Optics EXPRESS

In vivo photoacoustics and high frequency ultrasound imaging of mechanical high intensity focused ultrasound (HIFU) ablation

KHALID DAOUDI,[1,*] MARTIJN HOOGENBOOM,[2] MARTIJN DEN BROK,[3] DYLAN EIKELENBOOM,[3] GOSSE J. ADEMA,[3] JÜRGEN J. FÜTTERER,[2] AND CHRIS L. DE KORTE[1]

[1]*Department of Radiology and Nuclear Medicine, Medical UltraSound Imaging Centre, Radboud University Nijmegen Medical Centre, Netherlands*
[2]*Department of Radiology and Nuclear Medicine, Radboud University Nijmegen Medical Centre, Netherlands*
[3]*Department of Tumor Immunology, Radboud University Nijmegen Medical Centre, Netherlands*
**khalid.daoudi@radboudumc.nl*

Abstract: The thermal effect of high intensity focused ultrasound (HIFU) has been clinically exploited over a decade, while the mechanical HIFU is still largely confined to laboratory investigations. This is in part due to the lack of adequate imaging techniques to better understand the *in-vivo* pathological and immunological effects caused by the mechanical treatment. In this work, we explore the use of high frequency ultrasound (US) and photoacoustics (PA) as a potential tool to evaluate the effect of mechanical ablation *in-vivo*, e.g. boiling histotripsy. Two mice bearing a neuroblastoma tumor in the right leg were ablated using an MRI-HIFU system conceived for small animals and monitored using MRI thermometry. High frequency US and PA imaging were performed before and after the HIFU treatment. Afterwards, the tumor was resected for further assessment and evaluation of the ablated region using histopathology. High frequency US imaging revealed the presence of liquefied regions in the treated area together with fragmentized tissue which appeared with different reflecting proprieties compared to the surrounding tissue. Photoacoustic imaging on the other hand revealed the presence of deoxygenated blood within the tumor after the ablation due to the destruction of blood vessel network while color Doppler imaging confirmed the blood vessel network destruction within the tumor. The treated area and the presence of red blood cells detected by photoacoustics were further confirmed by the histopathology. This feasibility study demonstrates the potential of high frequency US and PA approach for assessing *in-vivo* the effect of mechanical HIFU tumor ablation.

OCIS codes: (170.0110) Imaging systems; (110.5120) Photoacoustic imaging; (170.7170) Ultrasound; (170.1020) Ablation of tissue.

References and links

1. L. Zhang and Z. B. Wang, "High-intensity focused ultrasound tumor ablation: review of ten years of clinical experience," Front. Med. China **4**(3), 294–302 (2010).
2. T. J. Dubinsky, C. Cuevas, M. K. Dighe, O. Kolokythas, and J. H. Hwang, "High-intensity focused ultrasound: current potential and oncologic applications," AJR Am. J. Roentgenol. **190**(1), 191–199 (2008).
3. G. T. Haar and C. Coussios, "High intensity focused ultrasound: physical principles and devices," Int. J. Hyperthermia **23**(2), 89–104 (2007).
4. K. F. Chu and D. E. Dupuy, "Thermal ablation of tumours: biological mechanisms and advances in therapy," Nat. Rev. Cancer **14**(3), 199–208 (2014).
5. H. Chen, A. A. Brayman, M. R. Bailey, and T. J. Matula, "Blood vessel rupture by cavitation," Urol. Res. **38**(4), 321–326 (2010).
6. H. L. Liu, Y. Y. Wai, W. S. Chen, J. C. Chen, P. H. Hsu, X. Y. Wu, W. C. Huang, T. C. Yen, and J. J. Wang, "Hemorrhage detection during focused-ultrasound induced blood-brain-barrier opening by using susceptibility-weighted magnetic resonance imaging," Ultrasound Med. Biol. **34**(4), 598–606 (2008).

#283510 https://doi.org/10.1364/BOE.8.002235
Journal © 2017 Received 26 Dec 2016; revised 8 Mar 2017; accepted 13 Mar 2017; published 20 Mar 2017

Biomedical Optics EXPRESS

7. F. Wu, Z. B. Wang, W. Z. Chen, J. Z. Zou, J. Bai, H. Zhu, K. Q. Li, C. B. Jin, F. L. Xie, and H. B. Su, "Advanced hepatocellular carcinoma: treatment with high-intensity focused ultrasound ablation combined with transcatheter arterial embolization," Radiology **235**(2), 659–667 (2005).
8. G. Aus, "Current status of HIFU and cryotherapy in prostate cancer--a review," Eur. Urol. **50**(5), 927–934 (2006).
9. X. L. Ren, X. D. Zhou, J. Zhang, G. B. He, Z. H. Han, M. J. Zheng, L. Li, M. Yu, and L. Wang, "Extracorporeal ablation of uterine fibroids with high-intensity focused ultrasound: imaging and histopathologic evaluation," J. Ultrasound Med. **26**(2), 201–212 (2007).
10. J. E. Parsons, C. A. Cain, G. D. Abrams, and J. B. Fowlkes, "Pulsed cavitational ultrasound therapy for controlled tissue homogenization," Ultrasound Med. Biol. **32**(1), 115–129 (2006).
11. W. W. Roberts, T. L. Hall, K. Ives, J. S. Wolf, Jr., J. B. Fowlkes, and C. A. Cain, "Pulsed cavitational ultrasound: a noninvasive technology for controlled tissue ablation (histotripsy) in the rabbit kidney," J. Urol. **175**(2), 734–738 (2006).
12. Z. Xu, Z. Fan, T. L. Hall, F. Winterroth, J. B. Fowlkes, and C. A. Cain, "Size measurement of tissue debris particles generated from pulsed ultrasound cavitational therapy-histotripsy," Ultrasound Med. Biol. **35**(2), 245–255 (2009).
13. T. D. Khokhlova, Y. N. Wang, J. C. Simon, B. W. Cunitz, F. Starr, M. Paun, L. A. Crum, M. R. Bailey, and V. A. Khokhlova, "Ultrasound-guided tissue fractionation by high intensity focused ultrasound in an in vivo porcine liver model," Proc. Natl. Acad. Sci. U.S.A. **111**(22), 8161–8166 (2014).
14. K. Daoudi, P. J. van den Berg, O. Rabot, A. Kohl, S. Tisserand, P. Brands, and W. Steenbergen, "Handheld probe integrating laser diode and ultrasound transducer array for ultrasound/photoacoustic dual modality imaging," Opt. Express **22**(21), 26365–26374 (2014).
15. M. Heijblom, D. Piras, M. Brinkhuis, J. C. van Hespen, F. M. van den Engh, M. van der Schaaf, J. M. Klaase, T. G. van Leeuwen, W. Steenbergen, and S. Manohar, "Photoacoustic image patterns of breast carcinoma and comparisons with Magnetic Resonance Imaging and vascular stained histopathology," Sci. Rep. **5**, 11778 (2015).
16. C. Lutzweiler and D. Razansky, "Optoacoustic imaging and tomography: reconstruction approaches and outstanding challenges in image performance and quantification," Sensors (Basel) **13**(6), 7345–7384 (2013).
17. L. V. Wang and S. Hu, "Photoacoustic tomography: in vivo imaging from organelles to organs," Science **335**(6075), 1458–1462 (2012).
18. P. V. Chitnis, H.-P. Brecht, R. Su, and A. A. Oraevsky, "Feasibility of optoacoustic visualization of high-intensity focused ultrasound-induced thermal lesions in live tissue," J. Biomed. Opt. **15**(2), 021313 (2010).
19. N. Dana, L. Di Biase, A. Natale, S. Emelianov, and R. Bouchard, "In vitro photoacoustic visualization of myocardial ablation lesions," Heart Rhythm **11**(1), 150–157 (2014).
20. H. Cui and X. Yang, "In vivo imaging and treatment of solid tumor using integrated photoacoustic imaging and high intensity focused ultrasound system," Med. Phys. **37**(9), 4777–4781 (2010).
21. J. P. Gray, N. Dana, K. L. Dextraze, F. Maier, S. Emelianov, and R. R. Bouchard, "Multi-Wavelength Photoacoustic Visualization of High Intensity Focused Ultrasound Lesions," Ultrason. Imaging **38**(1), 96–112 (2016).
22. M. Alhamami, M. C. Kolios, and J. Tavakkoli, "Photoacoustic detection and optical spectroscopy of high-intensity focused ultrasound-induced thermal lesions in biologic tissue," Med. Phys. **41**(5), 053502 (2014).
23. J. Shah, S. Park, S. Aglyamov, T. Larson, L. Ma, K. Sokolov, K. Johnston, T. Milner, and S. Y. Emelianov, "Photoacoustic imaging and temperature measurement for photothermal cancer therapy," J. Biomed. Opt. **13**(3), 034024 (2008).
24. M. Hoogenboom, M. J. van Amerongen, D. C. Eikelenboom, M. Wassink, M. H. den Brok, C. Hulsbergen-van de Kaa, E. Dumont, G. J. Adema, A. Heerschap, and J. J. Fütterer, "Development of a high-field MR-guided HIFU setup for thermal and mechanical ablation methods in small animals," J. Ther. Ultrasound **3**(1), 14 (2015).
25. M. Hoogenboom, D. Eikelenboom, M. H. den Brok, A. Veltien, M. Wassink, P. Wesseling, E. Dumont, J. J. Fütterer, G. J. Adema, and A. Heerschap, "In vivo MR guided boiling histotripsy in a mouse tumor model evaluated by MRI and histopathology," NMR Biomed. **29**(6), 721–731 (2016).
26. M. Hoogenboom, D. Eikelenboom, M. H. den Brok, A. Heerschap, J. J. Fütterer, and G. J. Adema, "Mechanical high-intensity focused ultrasound destruction of soft tissue: working mechanisms and physiologic effects," Ultrasound Med. Biol. **41**(6), 1500–1517 (2015).
27. PRIME, "Preclinical Imaging Centre, Radboudumc" https://www.radboudumc.nl/Research/Organisationofresearch/Departments/cdl/PRIME/Pages/default.aspx.
28. G. P. Luke, S. Y. Nam, and S. Y. Emelianov, "Optical wavelength selection for improved spectroscopic photoacoustic imaging," Photoacoustics **1**(2), 36–42 (2013).
29. S. Mallidi, K. Watanabe, D. Timerman, D. Schoenfeld, and T. Hasan, "Prediction of tumor recurrence and therapy monitoring using ultrasound-guided photoacoustic imaging," Theranostics **5**(3), 289–301 (2015).
30. Y. S. Hsiao, X. Wang, and C. X. Deng, "Dual-wavelength photoacoustic technique for monitoring tissue status during thermal treatments," J. Biomed. Opt. **18**(6), 067003 (2013).
31. K. Daoudi, P. van Es, S. Manohar, and W. Steenbergen, "Two-dimensional spatiotemporal monitoring of temperature in photothermal therapy using hybrid photoacoustic-ultrasound transmission tomography," J. Biomed. Opt. **18**(11), 116009 (2013).

Biomedical Optics EXPRESS

1. Introduction

The use of ultrasound (US) in clinical practice is no longer limited to diagnostic imaging and needle guidance in tumor biopsy, thanks to the possibility of using high intensity focused ultrasound (HIFU) which opened the door for promoting US as a non-invasive therapeutic method to treat different diseases [1,2]. US at high intensities is capable of producing both thermal and mechanical effects on tissue with non-invasive and selective destruction of a targeted tissue volume as a main advantages over other techniques allowing intactness of surrounding environment [3]. The thermal effect relies on temperature increase due to the absorption of US at the focal spot. This increase can vary depending on the intensity and treatment time leading to different stages of tissue destruction ranging from reversible heat induced injury (43 to 45 °C) to coagulation necrosis when the temperature exceeds 50 °C [4]. Mechanical effects induced by HIFU involves non-thermal tissue destruction and are associated with high intensity acoustic pulses, resulting in cavitations, micro-streaming, and radiation force leading to disruption of the vascular structure, connective tissue, and cellular damage [5, 6].

HIFU thermal ablation has been clinically applied for more than a decade to treat a wide variety of both benign and malignant tumors including uterine fibroids, prostate cancer, liver tumors and other solid tumors that are accessible to US energy [2, 7–9]. On the other hand, mechanical HIFU ablation techniques are still in an early stage of development mainly due to the poorly understood pathological and immunological effects caused by the treatment *in-vivo*. One of the mechanical ablation methods that have been investigated in recent years are cavitation cloud histotripsy and boiling histotripsy [10–13].

In boiling histotripsy we use millisecond ultrasound pulses with a duty cycle of less than 2% and acoustic powers which are generally five times as high as which are used for the thermal ablations. Using the high power, a shock wave and cavitation effects are taking place causing the targeted tissue to be fragmented into submicron sized fragments instead of thermal coagulation which occurs during thermal ablations [10–13]. The advantage is that the fragmented tissue can easily be absorbed as part of natural physiological healing responses. Furthermore, boiling histotripsy provides precise treatment localization. Compared to thermal ablation where thermal effect can affect surrounding tissue due to the thermal diffusion, mechanical ablation has limited impact on the surrounding since a sharp border between destructed and non-destructed tissue is created. Unfortunately, *in-vivo* reactions of this treatment are not well understood and the best way of treatment evaluation and non invasive monitoring is still under investigation. Therefore, there is a need for an adequate imaging technique to evaluate the effect of boiling histotripsy *in-vivo*. Additionally, to ensure the ablation is performed successfully and with the optimal outcome, the targeted region must be monitored non-invasively during and after the treatment. One of the main non-invasive methods that have been used to evaluate and monitor the ablation is US and magnetic resonance imaging (MRI) [2].

Recently photoacoustic imaging (PA) has gained tremendous interest among researchers and clinicians [14, 15] and might be an adequate candidate for this application. PA images the optical absorption of chromophores deep in highly scattering media. In this method, a short pulse of light is used to irradiate the sample of interest. The instantaneous absorption of energy by naturally occurring chromophores, or exogenous added dyes, induces a localized short temperature rise, which results in the generation of an US pulse via the thermoelastic effect. Using US detector placed outside the medium, the generated acoustic waves can be detected and by means of image reconstruction, the location of the US sources can be determined allowing for a two or three-dimensional visualization of the absorber distribution [16, 17]. Using PA as an alternative or add-on method to evaluate thermal HIFU treatment has been investigated in several studies [18–23], but to the best of our knowledge, it has never been used as a technique to evaluate mechanical ablation such as boiling histotripsy.

Biomedical Optics EXPRESS

The purpose of this feasibility study is to investigate the possibility of using PA and high-frequency US techniques to image *in-vivo* the effects of boiling histotripsy on tumor (neuroblastoma) mouse model. Recently, we set up and applied an MR guided mechanical HIFU approach for cancer ablation studies in mice [24–26] where we use extreme HIFU pressure to fragmentize the tissue into submicron fragments. In this work we make use of the high resolution of high frequency US to assess tissue structure and blood flow using Doppler and the high sensitivity of PA to red blood cells to monitor the destruction of blood vessel network. Three types of imaging modalities are used in this investigation: MRI to guide the HIFU ablation, US and PA to image *in-vivo* the tumor before ablation and evaluate the treated area after the ablation. The tumors, afterward, are resected and processed for histopathology to examine the treated area in term of lesion and content.

2. Materials and methods

2.1 Animal preparation

C57Bl/6n wild type mice were purchased from Charles River Wiga (Sulzfeld, Germany) and kept under specific pathogen-free conditions in the Central Animal Laboratory of the Radboud University (Nijmegen, the Netherlands). All animal experiments were performed according to the guidelines and by approval of the Nijmegen Animal Experiments Committee. The mice were subcutaneously injected with 0.5 × 10^6 9464D neuroblastoma tumor cells at the right femur.

Isoflurane gas at 3.5% was used for anesthetic induction. The anesthetic concentration was adjusted to 1–2% during the experiment in order to maintain the breathing frequency at 40–60 per minute. The body temperature was measured during the treatment using a rectal thermometer and maintained using a heated air flow device. In the PA/US imaging device, a heating plate was used to maintain the body temperature.

2.2 HIFU treatment

An MR compatible animal HIFU system (Image Guided Therapy—IGT, Pessac, France) was used in the experiment, Fig. 1(a). The trajectory of ablation was manually implemented based on MR imaging. A 16-channel annular array HIFU transducer, Fig. 1(b) with 3 MHz central frequency, 155-160 W acoustic peak power, 86.58° aperture, 48 mm diameter, adjustable focus depth 30–80 mm, was embedded in a positioning system (MR compatible piezoelectric motors, 30 × 30 mm trajectory execution range, active transducer cooling system) which was controlled by trajectory planner software (Thermoguide, IGT, Pessac, France). For good acoustic coupling of the US beam, the tumor area was shaved and the remaining hair was removed using standard hair removal cream. The mouse was positioned on top of an in-house made gel pad in lateral position, with the tumor inside a cavity (approximately 3.5 × 3.5 × 1 cm) made in the gel pad, and filled with degassed water [24].

2.3 Imaging protocol

The mice were first imaged before the treatment using high frequency US and PA imaging using a Vevo LAZR 2100 imaging system Fig. 1(c) equipped with an Nd:YAG laser capable of irradiating from 680 to 970 nm (FUJIFILM VisualSonics Inc., Toronto, Canada). Subsequently, the ablation took place in a 7T wide bore animal MR scanner where the ablated region was monitored using MR thermometry during the treatment. An in-house built surface coil was positioned around the tumor. Mice were treated with boiling histotripsy: a pulsed wave method utilizing 5ms pulses with an acoustic output power of 160 Watt, pulse repetition frequency of 1Hz and 200 pulses per focal spot. A total of 25 spots for mouse 1 and 16 spot for mouse 2 (focal size 0.5x0.5x2.0 mm) were focused 1 mm apart in one plane.

Biomedical Optics EXPRESS

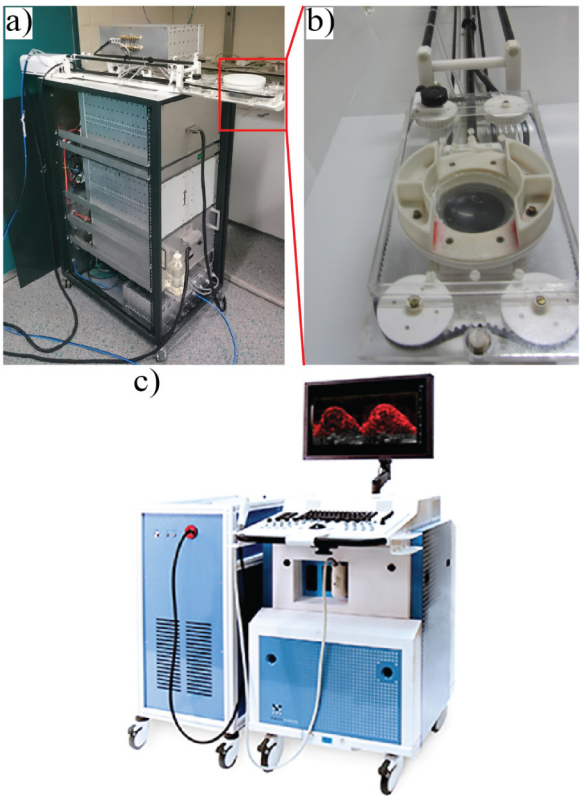

Fig. 1. Pictures of the HIFU and imaging system used in the experiment, (a) MR compatible animal HIFU system, (b) zoomed image on the 16-channel annular array HIFU transducer used for the ablation, (c) Vevo LAZR 2100 system for high frequency US and PA imaging.

After the treatment T2 weighted and enhanced contrast MR images were made for treatment evaluation as described in our previous study [25]. Then the mice went again for US and PA imaging. The ultrasound images were obtained using 40 Mhz central frequency transducer while PA was performed using 21 Mhz central frequency transducer. In the PA experiment, we used 4 wavelengths in the near infrared region (730, 760, 800 and 850 nm). Imaging with different modalities was facilitated by PRIME at Radboudumc [27], a center which hosts a multitude of imaging modalities. The treated tumors were finally resected and processed for histopathology for further analysis.

3. Results

3.1 Ultrasound imaging

Figure 2 shows US images of the tumor of mouse 1 and 2 respectively before Figs. 2(a) and 2(b) and after Figs. 2(c) and 2(d) the mechanical HIFU treatment where the orange dotted line delineates the treated region. In the post-treatment images Figs. 2(c) and 2(d) an echoic region with a tissue texture different from the surrounding tissue can be discerned. The region is composed of a slightly hyperechoic region (green arrow) caused by fragments of cells and collagen debris generated from the boiling histotripsy and a hypoechoic region (red arrow) revealing the presence of liquefied region caused by the complete pulverization of the tumor cells, and intact cells outside the treated area (yellow arrow). In histopathology, we can distinguish the presence of accumulated fragmented tumor cells, chromatin and collagen debris in mouse 1, Fig. 2(e) as well as the presence of red blood cells delineated with a blue dotted line in the zoomed image. The histopathology image of mouse 2 showed a completely

Biomedical Optics EXPRESS

liquefied region with very little red blood cells Fig. 2(f) and collagen more accumulated near the border of the lesion. Histopathology shows also sharp borders between treated region (green and red arrows) and untreated region (yellow arrow), no viable tumor cells were found in the treated region in both mice.

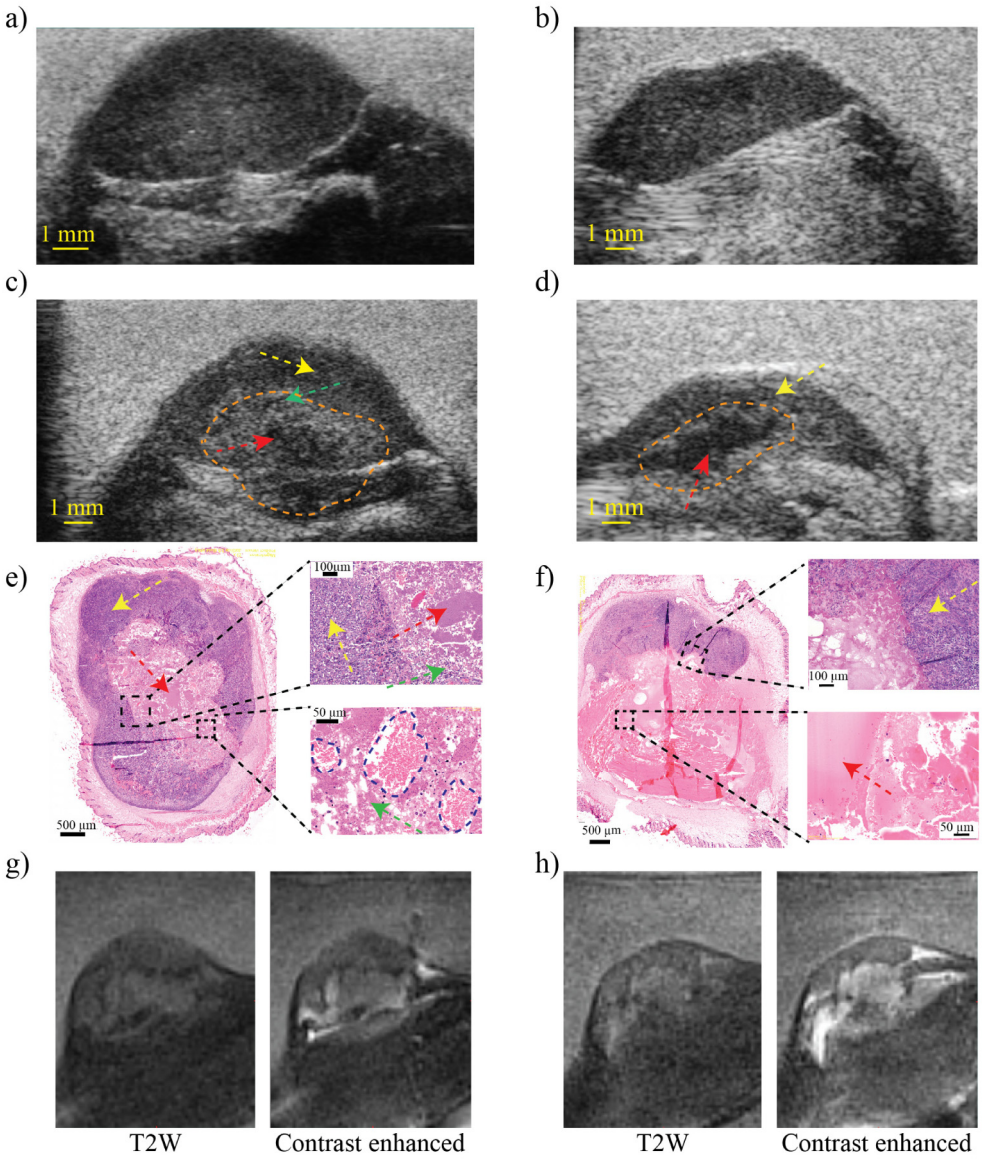

Fig. 2. High-frequency ultrasound images before (a), (b) and after treatment (c), (d) of mouse 1 and 2 respectively using 40 Mhz ultrasound transducer. (e) and (f) represent the histopathology of one slide of the tumors after treatment with 2 zoomed regions each. The green arrow indicates the fragments of tumor cells, the red arrow indicates liquefied region, yellow arrow indicates non treated tumor region and red blood cells are delineated with a blue dotted line in the zoomed region of panel (e). (g) and (h) are MR images of mouse 1 and 2 respectively, left image is T2W images and right is contrast enhanced images.

Since the treatment was performed under MRI guidance, normal T2W and contrast-enhanced MR Images were obtained. Figures 2(g) and 2(h) shows the MR images of mouse 1 and mouse 2 respectively. T2w images (left images) reveal the treated region due to the hypo-

Biomedical Optics EXPRESS

intense border between the treated area and untreated area. Using contrast-enhanced imaging (right images) an indication could be made of the leakage of blood vessels due to the presence of the contrast in the treated area.

Furthermore, we investigated blood vessel network distribution within the tumor before and after ablation. Figure 3 presents the 3D color Doppler images obtained for both mice. Figures 3(a) and 3(b) represent the blood vessel network of mouse 1 and 2 respectively before the treatment and Figs. 3(c) and 3(d) are obtained post-treatment. In both mice, color Doppler imaging revealed the disappearance of the blood vessel network after the treatment either completely, for mouse 1, or partially for mouse 2 where few vessels were still visible at the side of the tumor in the untreated part.

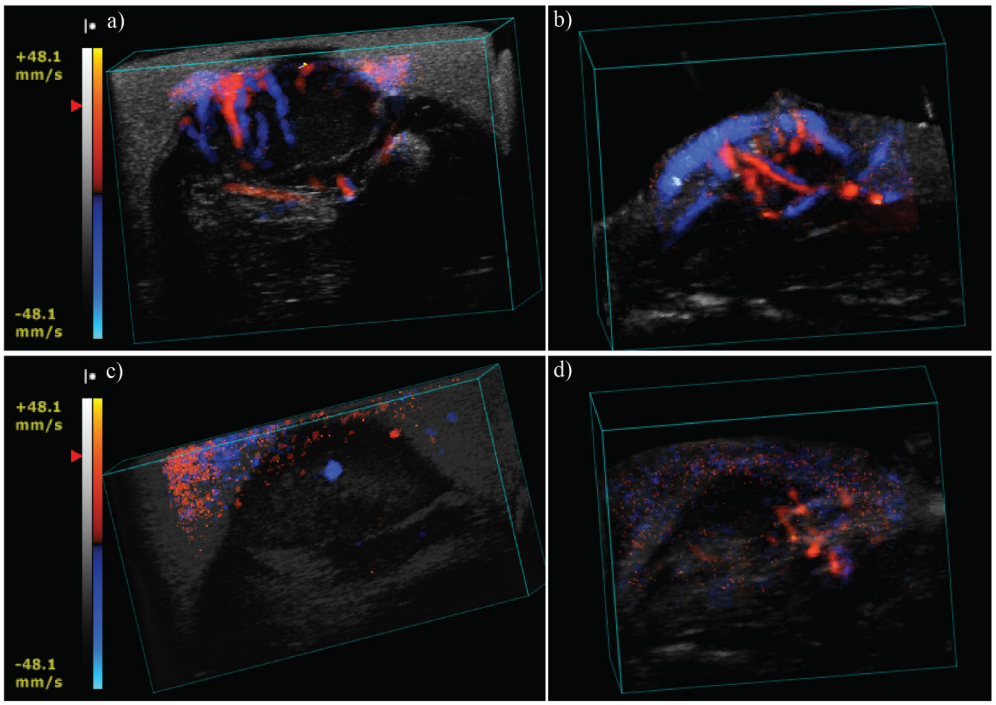

Fig. 3. Ultrasound color Doppler of mouse 1 and 2 before treatment (a) and (b) and after treatment (c) and (d) respectively

3.2 Photoacoustic imaging

Figure 4(a) represents the PA image of mouse 1 before treatment and 4(b) after treatment. Pre-treatment PA imaging identifies an absorbing skin layer and absorbing structures at different locations within the tumor corresponding to blood vessels. Post-treatment, a large absorbing structure with higher signal intensity not visible before the treatment was detected. This new and overwhelming signal is most likely caused by the presence of blood hemorrhage within the tumor due to the blood vessel destruction. The presence of blood was supported by the histopathology as can be seen in the previous Fig. 2(e) (the zoomed region). Aggregated red blood cells are present in the treated part of the tumor, delineated with a blue dotted line, scattered in between fragmented cell material. The presence of hemorrhage is likely caused by rupturing of blood vessels due to the treatment.

Using photoacoustic spectroscopy (PAS) and least-squares fitting algorithm to unmix the images [28] we can reveal the nature of the blood present in the tumor before and after the treatment. Figure 4(c) shows the unmixed image before the ablation where we see predominantly the presence of oxygenated vessels within the tumor, whereas Fig. 4(d) shows

Biomedical Optics EXPRESS

the unmixed image after the ablation which revealed the presence of deoxygenated red blood cells inside the treated region. This result corresponds to what one would expect from hemorrhage presence following blood vessel disruption.

On the other hand pre-treatment PAS imaging of mouse 2 revealed the presence of oxygenated and deoxygenated blood vessels inside the tumor Fig. 4(e), while, post-treatment imaging Fig. 4(f) showed very little deoxygenated blood signal compared to mouse 1. The low red blood cell signal detected in the treated area of mouse 2 is likely due to the complete pulverization of the cells within the ablated region and the absence of hemorrhage unlike mouse 1. Histopathology images Fig. 2(f) showed that a larger liquefied region surrounded by intact tissue has resulted from the ablation with a little presence of red blood cells in the treated region.

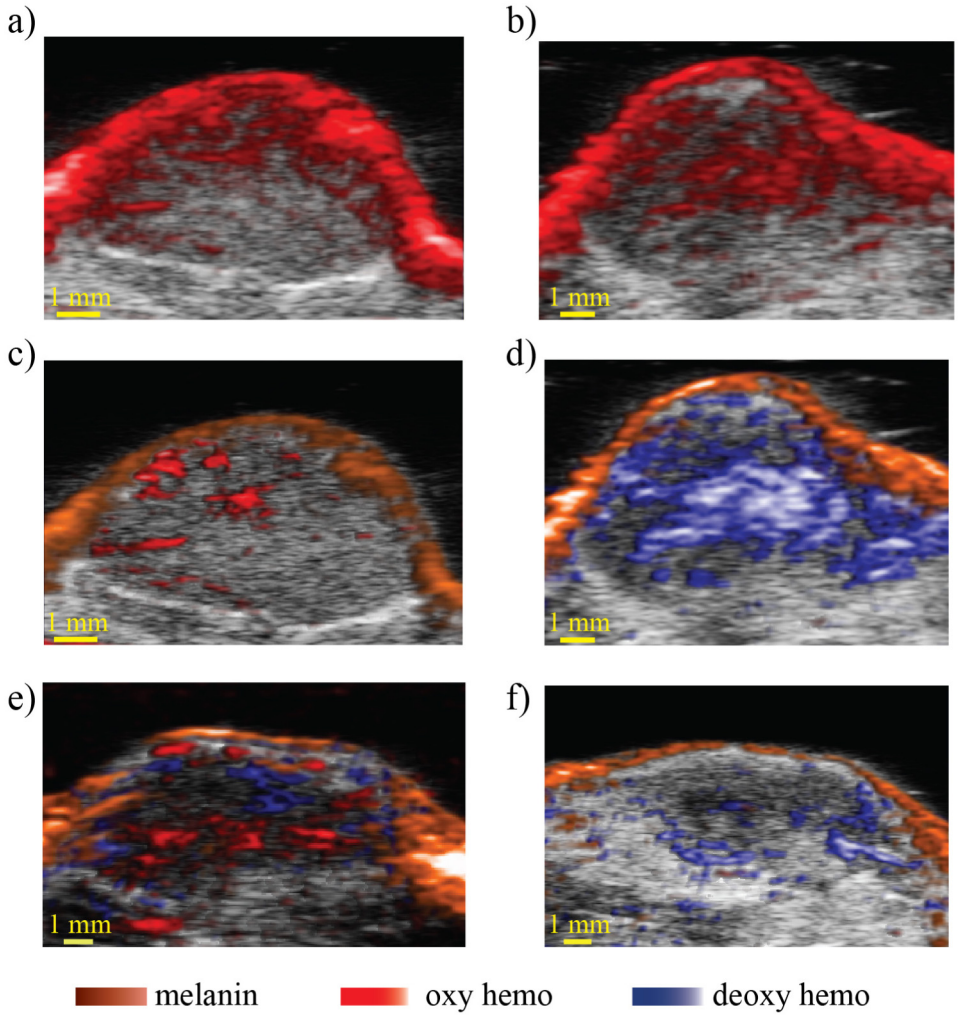

Fig. 4. (a) and (b) pre and post treatment photoacoustic images of mouse 1, (c) and (d) are the corresponding unmixed images using melanin, deoxy and oxy hemoglobin spectra, (e) and (f) are unmixed images of mouse 2 using the same spectra before and after the ablation respectively.

Biomedical Optics EXPRESS

4. Discussion and conclusion

Mechanical HIFU ablation of tumors has the potential to become a major therapeutic means in oncology and preclinical investigations are essential to fill the gap in our understanding of its pathological and immunological effects *in-vivo*. Several mechanical effects can be created by HIFU ablation depending on the treatment settings. Here, we investigated mechanical HIFU using our recently established setting for boiling histotripsy [24, 25]. This relatively new technique uses extremely high US pressure to destroy and pulverize the targeted tissue. Understanding the impact on pathology and long term recovery as well as the consequences for the immune system is a necessity. To tackle this lack of comprehension, we need to study *in-vivo* and non-invasively the effect in different aspects using an adequate real-time imaging modality.

In this feasibility study, we investigated multimodal imaging to detect different effects caused by the boiling histotripsy ablation. For the purpose of the study, two mice were prepared and injected with neuroblastoma tumor cells in the right leg and both were treated with high-pressure amplitudes. We utilized PA imaging with co-registered high frequency US to non-invasively image the tumor before and after HIFU ablation.

Using the PA technique, which is mainly sensitive to blood, we observed the appearance of a large absorbing structure in the treated region of mouse 1 while before the treatment we saw signals related to the presence of blood vessels inside the tumor Fig. 4. This observation was confirmed using histopathology with clear appearance of red blood cells in many parts of the treated region. However, point-by-point comparison between histopathology and PA images cannot be made here due to the spatial resolution difference between the imaging modalities and due to a different PA imaging plane orientation in this experiment with respect to the histopathology sections. PAS further allowed extracting the blood characteristics, which was classified as deoxygenated post-treatment while the detected vessels were mainly oxygenated before the treatment. The deoxygenation can be explained by the presence of red blood cells outside the vessels due to their rupture or destruction as a result of the ablation. The information about the oxygenation of the ablated region can be crucial in the prediction of the outcome after ablation. In fact it has been shown, for example in photodynamic therapy, that the remaining oxygenated parts of the tumor after the treatment had more chance of tumor recurrence than deoxygenated parts [29]. This demonstrates the importance of monitoring oxygenation during and after the treatment which will be performed in future study. In the case of mouse 2, red blood cells were less present after the treatment due probably to the complete destruction of the blood vessels and pulverization of the cells while pre-treatment imaging showed both oxy- and deoxygenated blood vessels within the tumor. Histopathology images confirmed the absence of blood cells and a large liquefied region in the treated area.

In this study we used C57bl/6 black mice for proof of principle, which may explain the high signal generated by the skin due to the high concentration of the melanin. In future studies the use of non-pigmented mice should improve the PA signal generation within the tumor.

The treatment followed a predefined path in MRI-HIFU system and the same pressure amplitude and the same number of pulses were applied in each position of the scan for both mice. Although both mice were successfully treated and no intact tumor cells were seen inside the ablated area, the high resolution of high frequency US imaging revealed different structures in both mice. The high frequency US images of the mouse 2 have shown the treated area composed of large hypoechoic region revealing the liquid nature of the ablated region. The histopathology study confirmed the US findings and revealed the ablated region to be composed of a completely liquefied region containing emulsified tumor debris and probably edema. Images of mouse 1 revealed a region with mainly hyperechoic structure caused by regions with accumulation of larger fragments of pulverized cells and red blood cells which leaked out from ruptured vessels. MRI, on the other hand, allowed detecting the treated area

Biomedical Optics EXPRESS

using T2w and contrast enhanced imaging. However compared to ultrasound, MR images looked similar in both mice which shows its limitations to distinguish the nature of the ablation and whether the treated cells were completely fragmented or not. Furthermore, the MR images were not suitable to determine the amount of fragmentation as well as to differentiate between edema effects or major hemorrhage which was possible with PA due to its sensitivity to red blood cells allowing the detection of hemorrhage within the treated area and revealing its oxygenation status. A study including a larger number of mice will be needed to address to what extend high frequency US imaging and PA can be used to more precisely monitor ablation efficacy by mechanical HIFU treatment beyond the sensitivity of MRI and to thoroughly investigate the differences in fragmentation and hemorrhage between mice.

The treatment destroyed the blood vessels within the tumor as evidenced by color Doppler images Fig. 3. The figures have shown clear differences in blood vessel network before and after treatment in both tumors. Most of the detected vessels before the treatment were not any longer visible after the ablation. In this study, the mice were treated in an MRI-HIFU system and imaged using Vevo 2100 system. We are aware that moving the mouse in between imaging set-ups may affect the result, especially US Doppler imaging where the orientation is crucial. However, since we acquired 3D US, color Doppler and PA data of the whole tumor, co-registration of the treatment region as assessed with MRI and the US-based data was facilitated. Consequently, we were able to reproduce the same configuration before and after the treatment. Future work will focus on performing the HIFU ablation within the Vevo system in order to monitor the mice during the treatment. In fact PA and US can also be used as a method to monitor temperature increase during thermal treatment [23, 30, 31]. This will allow avoiding any interpretational errors which may be caused by using a different HIFU guided system.

This feasibility study proves that the combination of PA and high frequency US imaging can be a powerful tool to better understand the effect of boiling histotripsy. While US gives an indication of the anatomy and the nature of the lesion and color Doppler reveals the vasculature, PA will provide more insights in the presence of blood in vessels or in the liquefied region and the oxygenation state of the blood in the tumor using spectroscopy. The results presented here will act as a baseline for a larger follow-up study to improve the HIFU treatment, to monitor tumor response over time such as regrowth of blood vessels and the long term ablation outcome and to investigate the physiological effects of the treatment.

Funding

This work was supported by a RadboudUMC PhD grant.

Acknowledgment

Authors would like to thank Visualsonics, Inc. for their support